$r_1', r_2' = r_1/\bar{r}, r_2/\bar{r}$
R = propellor radial coordinate or radius of turbulent eddy
R' = R/R_a
R_a = radius of propellor
R_m = maximum eddy size which is turbulent relative to obstacle
S = characterizes crystal surface morphology, nuclei/unit driving force
t_g, T_g = functions defined after Equation (12)
t_t, T_t = functions defined after Equation (13)
ΔT = solution subcooling
$v(r_1, r_2)$ = velocity of crystal radius r_1 relative to crystal radius r_2
v_c = collision velocity
v_s = velocity of fluid relative to blade element
V_c = volume of crystallizer
W = half width of blade element
x = weight fraction of crystals, Kg(crystal)/Kg(total)

Greek Letters

α = hydrodynamic angle
β = nucleation rate per crystal, nuclei/crystal · s · m^3
ϵ = square of collision velocity normalized with respect to $v_s \sin\alpha$
ϵ_t = square of collision velocity, m/s^2
η = collection efficiency of blade element
η_p = collection efficiency of propellor
θ = angle of propellor blade relative to the plane of the propellor
μ = dynamic viscosity
$\mu_n = \int_0^\infty r^n f(r)\, dr$
ρ = distance of crystal from obstacle
ρ_f = density of fluid
ρ_i = density of crystal
ϕ = solid angle for crystal colliding with obstacle
ϕ_c = maximum solid angle
ω = collision frequency, collision/crystal · s

Subscripts

b = crystal-crystallizer collisions driven by the bulk flow
ct = crystal-crystallizer collisions driven by turbulence
g = crystal-crystal collisions driven by gravity
t = crystal-crystal collisions driven by turbulence

LITERATURE CITED

Brian, P. L. T., H. B. Hales and T. K. Sherwood, "Transport of Heat and Mass Between Liquids and Spherical Particles in an Agitated Tank," *AIChE J.*, **15**, 727 (1969).

Brian, P. L. T., A. F. Sarofim, T. W. Evans, and S. G. Kane, "The Kinetics of the Secondary Nucleation of Ice: Implications to the Operation of Continuous Crystallizers", submitted to *Desalination* (1974).

Brothman, A., A. P. Weber, and E. Z. Barish, *Chem. Metal. Eng.*, **50**, 107 (1943).

Clontz, N. A., and W. L. McCabe, "Contact Nucleation of Magnesium Sulfate Heptahydrate," *Chem. Eng. Progr. Symp. Ser. No. 110*, **67**, 6 (1971).

Evans, T. W., "Mechanisms of Secondary Nucleation during the Crystallization of Ice," Ph.D. thesis, M.I.T., Cambridge, Mass. (1973).

———., G. Margolis, and A. F. Sarofim, "Mechanisms of Secondary Nucleation in Agitated Crystallizers," *AIChE J.*, **20**, (1974).

Grant, H. L., R. W. Stewart, and A. Moilliet, "Turbulence Spectra from a Tidal Channel," *J. Fluid Mech.*, **12**, (2), 241 (1962).

Hinze, J. O., *Turbulence*, McGraw-Hill, New York (1959).

O'Brien, T. P., *The Design of Marine Screw Propellors*, Hutchinson & Co., Ltd., London (1962).

Ottens, E. P. K., A. H. Janse, and E. J. deJong, "Secondary Nucleation in a Stirred Vessel Cooling Crystallizer," *J. Crystal Growth*, **13/14**, 500 (1972).

Ottens, E. P. K., and E. J. deJong, "A Model for Secondary Nucleation in a Stirred Vessel Cooling Crystallizer," *Ind. Eng. Chem. Fundamentals*, **12**, 179 (1973).

Wadia, P. H., "Mass Transfer from Spheres and Discs in an Agitated Tank," Sc.D. thesis M.I.T., Cambridge, Mass. (1974).

Manuscript received November 9, 1973; revision received May 24 and accepted May 30, 1974.

Experimental Investigation of Polarization Effects in Reverse Osmosis

With a Mach-Zehnder interferometer, salt concentration profiles were measured in a reverse osmosis system under natural convection with the membrane in a vertical position. The measured concentration profiles compared favorably with those predicted theoretically as long as the motion remained laminar. At large distances from the leading edge, however, the flow developed a wavy pattern, especially for bulk salt concentrations in excess of 0.1 moles/liter. As expected, whenever this motion became especially pronounced, the concentration of salt at the membrane surface was less and the production rate of fresh water greater than that predicted using the laminar analysis.

A. R. JOHNSON

Department of Chemical Engineering
Stanford University
Stanford, California 94305

SCOPE

One of the more promising techniques of desalination is the so-called "reverse osmosis" process, in which separation is accomplished by applying sufficient pressure to a salt solution to force the water through a semipermeable membrane, that is, a membrane that will preferentially allow the passage of water molecules over salt ions. The process suffers from the fact, however, that as the water

A. R. Johnson is with Kaiser Aluminum & Chemical Company, Permanente, California 95014.

is forced through the membrane an increase in the salt concentration of the solution takes place near the membrane surface. This reduces the effectiveness of the system by lowering the production rate and increasing the product salt concentration.

To prevent the water flux from decreasing with time due to this increased concentration, or polarization, it is then necessary to remove this more concentrated solution from the region adjacent to the surface of the membrane, for example, by pumping fresh solution under pressure past the membrane surface. Dresner (1963), Sherwood et al. (1965), Gill et al. (1966), and Hendricks and Williams (1971) have investigated the effects of forced convection in reverse osmosis and have shown that, as expected, these can substantially diminish the degree of polarization.

In previous investigations it was customary to measure the product concentration and water flow rate and then to determine analytically the concentration polarization using a mathematical model of the experimental set-up consisting of the Navier-Stokes and diffusion equations together with appropriate boundary conditions. It remained to be shown, however, that the solution to these equations accurately described the polarization in the system in question. For example, as is often the case in hydrodynamics, the mathematical system governed by the steady state equations might be an unstable one, hence the flow structure, and thus the polarization might be quite different from that predicted on the basis of a steady state analysis. It is necessary, therefore, to determine experimentally the actual concentration profiles to see whether or not the model proposed for the system is a valid one and can be used with confidence.

To date, the only previous experimental studies of the concentration polarization appear to be those by Hendricks and Williams (1971), who measured concentration profiles in a forced convection configuration, and by Liu and Williams (1970), who made these measurements in an unstirred batch cell. The present work deals with a natural convection system in which fluid motion is imparted by the difference in density between the bulk fluid and the more concentrated, and hence heavier, solution near the surface of the membrane. Measurements of the concentration profiles in this case were made using a Mach-Zehnder interferometer, utilizing the change in refractive index due to the polarization near the membrane.

The natural convection set-up is somewhat similar to forced convection, which, as mentioned above, has already been studied both theoretically and experimentally, besides being used in commercial desalination facilities utilizing reverse osmosis. However, the advantage of natural convection for the purposes of this work is that the system is considerably easier to handle, when compared to the corresponding forced convection case, in that the elaborate circulating system complete with high pressure pump and channel for fully developed flow is eliminated. Instead all that is required is a vessel to house the osmotic membrane and salt solution and a source of compressed gas to develop the necessary pressure driving force.

CONCLUSIONS AND SIGNIFICANCE

The main results of this work are the following:

1. The proposed mathematical model can be used with confidence to predict accurately the concentration polarization in a reverse osmosis apparatus under conditions of natural convection, provided the flow remains laminar. Moreover, in view of the similarity between forced and free convection, it would appear likely that the laminar theory, when properly extended, should also be expected to apply in a forced convection system.

2. In natural convection, at some distance from the leading edge of the flat plate, a wavy motion results that would make this system more useful in reverse osmosis if the resulting decrease in concentration polarization were large enough. Quantitative measurements of the polarization when the unsteady motion was most pronounced could not be made with the interferometer since the concentrations under these conditions were too large to allow resolution of the fringe shift. However, measurements of the flow rate showed that when the osmotic pressure was of the same order as the applied pressure, the experimentally determind flow rates were significantly greater than those predicted theoretically using a laminar analysis. For greater applied pressures, which correspond to the more practical operating conditions, there was little difference between the theory and the experiments.

3. The Mach-Zehnder interferometer proved to be a very useful and reliable instrument for this type of work. The main limitation of the interferometer is that the more concentrated solutions (bulk concentrations greater than 0.1 moles/liter) make resolution of the fringe shift difficult, if not impossible, and may lead to problems due to the deflection of the light beam.

It was the purpose of this study to demonstrate the conditions, if any, under which a mathematical model of a reverse osmosis system could be used to predict accurately the concentration polarization and thus the performance of the desalination process. The results clearly indicate that the laminar flow model is representative of the actual polarization that exists in the system in question. Under conditions of turbulent flow, while the laminar theory overestimates the degree of polarization, the contribution of the polarization to the overall driving force for the reverse osmosis process is small in practical applications.

THEORETICAL DISCUSSION

In the natural convection system the membrane can be thought of as a vertical plate for which the flux at the surface is nonzero. Figure 1 gives a schematic diagram of this system, showing the coordinate axes and the two components of the velocity. The velocity component u' is imparted and sustained by the buoyancy force produced by the increased salt concentration at the surface of the membrane.

As was shown by Johnson and Acrivos (1969), the dimensionless momentum and diffusion equations for this system reduce to the familiar laminar boundary layer equations for natural convection heat transfer to a high Prandtl number fluid (Acrivos, 1960)

$$\partial^2 u/\partial y^2 + \theta = 0 \qquad (1)$$

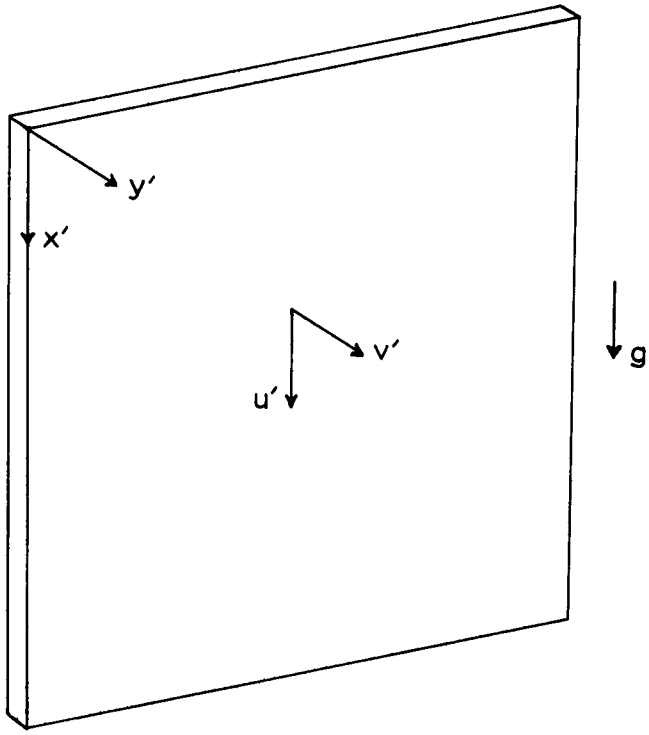

Fig. 1. Schematic of vertical flat plate.

$$\partial P/\partial y = 0 \tag{2}$$

$$u\,\partial\theta/\partial x + v\,\partial\theta/\partial y = \partial^2\theta/\partial y^2 \tag{3}$$

provided that $N/Sc^2 >> 1$ and $Sc >> 1$. Since for a typical reverse osmosis system, for example, salt and water, N is $0(10^9)$ and Sc is $0(10^3)$, these inequalities are generally satisfied.

The requirements that the total flux of salt at the surface be equal to the salt flux penetrating the membrane and that the velocity u' be zero at the surface of the plate lead to the boundary conditions

$$v_s = \frac{1}{R(1+\theta_s)}\left(\frac{\partial\theta}{\partial y}\right)_{y=0} \tag{4}$$

$$u = 0 \quad \text{at} \quad y = 0 \tag{5}$$

respectively. R, the salt rejection coefficient, is defined by

$$R \equiv 1 - c_p/c_s \tag{6}$$

For simplicity it will be assumed that R is independent of solute concentration. Although Sourirajan (1970) has developed an alternative approach making this assumption unnecessary, for dilute solutions (less than 1 mole/liter) the concentration dependence of R can be neglected with little error (Agrawal and Sourirajan, 1969).

The water flux through the membrane is described by the relationship (Merten, 1963)

$$v_s = -\,(1 + \alpha(1-R) - \alpha R\theta_s) \tag{7}$$

Equations (1) to (3) apply, of course, only within the diffusion layer and are not valid at large distances from the plate surface where the effects of the inertia terms must be considered (Stewartson and Jones, 1957). However, when the solution appropriate in the outer region is matched to that from the inner region according to the standard requirements of the method of inner and outer expansions, it is found (Johnson, 1970) that the solution in the diffusion layer for large Sc becomes uncoupled from that in the outer region and that the appropriate boundary conditions as $y \to \infty$ become

$$\left(\frac{\partial u}{\partial y}\right)_{y\to\infty} = 0 \tag{8}$$

$$\theta(x, \infty) = 0 \tag{9}$$

As shown by Johnson and Acrivos (1969), the above system of equations can be reduced to a set of ordinary differential equations by expanding the dependent variables about the leading edge of the plate. This expansion takes the form

$$u = x^{3/5} \sum_{n=0}^{\infty} x^{n/5} f_n'(\eta) \tag{10}$$

$$\theta = x^{1/5} \sum_{n=0}^{\infty} x^{n/5} \phi_n(\eta) \tag{11}$$

which, when substituted into (1) to (3), yields an infinite system of ordinary differential equations for the functions f_n and ϕ_n. In turn, these can be solved numerically using the standard Kutta-Merson technique (Fox, 1962) for given values of the parameters α and R.* The first set of equations is nonlinear and homogeneous; the remainder are all linear and nonhomogeneous. These equations and their boundary conditions, together with the techniques used to find their solution, are presented in detail by Johnson (1970).**

The concentration profile at any given value of x can be evaluated from (11) as a function of y or η and compared with that obtained experimentally. Also, using the calculated results for the polarization, it is possible to compute the overall flow rate Q of solvent through the entire plate, where

$$Q = -\int_0^{L'} b v_s'(x')\,dx' \tag{12}$$

In view of (7), the above becomes

$$Q = Q_0 - h\int_0^L \theta_s\,dx \tag{13}$$

Finally, because of (11)

$$\theta_s = x^{1/5} \sum_{n=0}^{\infty} x^{n/5} \phi_n(0) \tag{14}$$

hence (13) reduces to

$$Q = Q_0 - h \sum_{n=0}^{\infty} \frac{5}{n+6} L^{(n+6)/5} \phi_n(0) \tag{15}$$

The flow rate Q can now be calculated from (15) and compared to the experimental measurements.

EXPERIMENTAL APPARATUS

Measurements of the concentration polarization were made using a Mach-Zehnder interferometer with a helium-neon laser as a light source. The principal features of the Mach-Zehnder interferometer have been described in detail by Ladenburg and Bershader (1954). In the present case the increased concentration near the membrane surface caused a change in refractive index, which, in turn, led to a shift in the interference fringes produced by the interferometer.

* The solution to the special case $R = 1$ was developed previously by Johnson and Acrivos (1969).

** The Supplement has been deposited as Document No. 02463 with the National Auxiliary Publications Service (NAPS), c/o Microfiche Publications, 305 E. 46 St., N.Y., N.Y. 10017 and may be obtained for $1.50 for microfiche or $5.00 for photocopies.

The details of the construction and operation of the interferometer are given by Johnson (1970).

The osmotic membranes used in the experiments were composed essentially of cellulose acetate, acetone, water, and magnesium perchlorate, and were obtained from Gulf General Atomic's reverse osmosis division in San Diego, California. These membranes, which are about 0.10 mm in thickness, have basically a two-layered structure; the top layer is thin and very dense and comprises less than 1% of the total membrane thickness, while the reaminder consists of a porous substructure.

The design of the vessel to support and house the osmotic membrane was based on the requirements of the natural convection model. A diagram of this vessel with all its various components is shown in Figure 2. When placed in the upright position, the surface of the membrane was vertical and acted as a vertical flat plate, as in the mathematical model. The vertical plate was 910 cm long and 9.9 cm wide, which was wide enough to assure two-dimensionality in natural convection, the ratio of the diffusion layer thickness to the plate width being about 1:100. The sides of the vessel were far enough from the edges of the plate (about 12.5 mm) relative to the diffusion layer thickness to eliminate any wall effects.

Two pairs of windows (two on each side of the vessel) were used in order to view the surface of the membrane from the plate edge in the interferometer. The first set was located about 15 cm from the leading edge of the vertical plate, that is, far enough from the leading edge where the theoretical solution developed above is invalid owing to the fact that the derivative $\partial^2/\partial x^2$ is of the same order as $\partial^2/\partial y^2$ and can no longer be neglected in Equations (1) and (3). The radius of this region is $O(D/A\Delta P)$ (Johnson, 1970), or for the typical NaCl-water system used here, approximately 1 cm or less. The second set of windows was located at about 60 cm from the leading edge.

The entire system was pressurized with a cylinder of compressed air. A calibrated pressure gauge was used, which could be read to the nearest lb./sq.in. with a maximum scale deflection of 400 lb./sq.in.

Any measurement of feed (or product) concentration was made by determining the electrical resistance of the solution in a dip-type conductivity cell (Chiu and Fuoss, 1968; Daniels et al., 1962).

A detailed discussion of the experimental equipment is given by Johnson (1970).

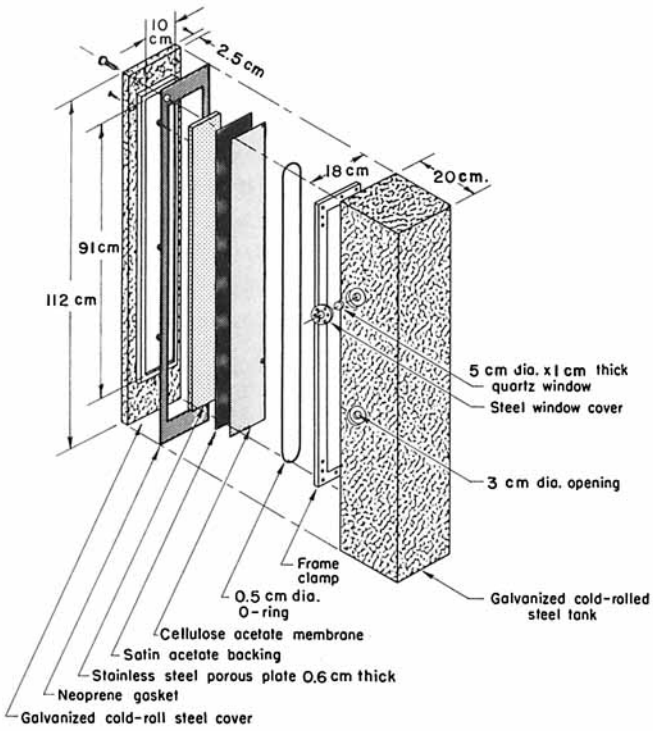

Fig. 2. Diagram of vessel housing osmotic membrane.

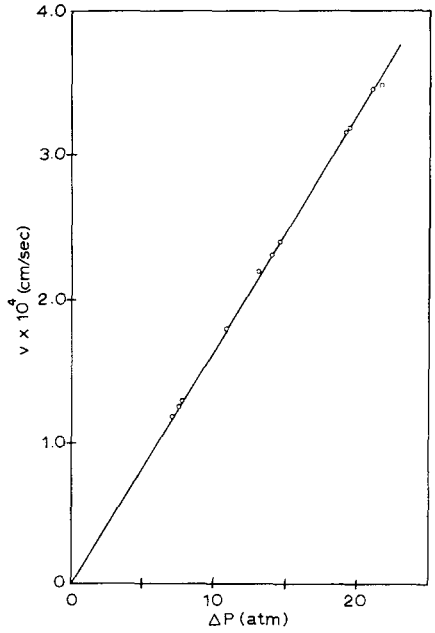

Fig. 3. Product velocity through membrane vs. applied pressure for distilled water. Slope of line gives $A = 1.62 \times 10^{-5}$ cm/s-atm.

RESULTS

Membrane Constant Measurements

In the tests to determine the membrane constant, the vessel was filled with distilled water so that the osmotic pressure term could be neglected in Equation (7). The velocity v_s was then found by measuring the volumetric flow rate of the water through the membrane for various applied pressures and dividing it by the membrane area of 900 cm^2. Figure 3 depicts the results of one representative test, with A given by the slope of this line. The values of A ranged from 0.8×10^{-5} to 1.8×10^{-5} cm/s-atm for one roll of membrane, compared to the manufacturer's quoted value of 1.3×10^{-5} cm/s-atm. Since the membrane may compact when used under pressure and thereby lead to a decrease in the flow rate with time, measurements of A were taken before and after each test, and an average value was used to represent the experimental condition.

Salt Rejection Measurements

The salt rejection coefficient R is a parameter that must be known before the concentration polarization can be evaluated. This coefficient was determined by using the vessel in a horizontal position, with the rejection surface facing up, to simulate a batch cell configuration.

The batch cell system is inherently a transient process, with the polarization increasing with time. Raridon et al. (1966) developed a solution for the case $R \neq 1$. For large values of their parameter τ (dimensionless time), it can be shown from their Equation (21) that a steady state condition can be approached in which the flow rate becomes constant, and all the salt convected to the membrane surface passes through the membrane. Consequently, in such a case, c_p will equal the bulk concentration c_x.

This last result does not apply, however, if the surface concentration increases to such a large extent that, during the process, the osmotic pressure of the solution at the membrane surface becomes equal to the applied pressure. In this case the product flow would asymptotically approach zero with time. Specifically, if we set $c_p = c_x$, we have from the definitions of R and θ, that $\theta_s = R/(1 - R)$, hence, from (7),

$$v_s = -1 + \alpha(2R - 1)/(1 - R) \qquad (16)$$

Clearly then the asymptotic solution in which $c_p = c_\infty$ applies only if $\alpha(2R - 1)/(1 - R) < 1$. This condition was satisfied by using dilute solutions so that $\alpha << 1$.

Experimentally, the surface concentration c_s was measured with the interferometer after the product concentration had reached its asymptotic value. The product water flow rate did decrease during the course of the batch cell tests, but the ratio of the final to the initial flow rate was between 0.90 and 0.98 in most cases. Clearly, the contribution of the osmotic pressure term due to polarization in Equation (7) was small.

The deviation between c_p and c_x was often quite large, with the average deviation of their ratio from 1 being 0.2 and the standard deviation 0.25. The reason for this discrepancy was probably due to such factors as membrane fouling, small membrane punctures, and nonuniformities in the membrane surface.

Despite the discrepancy between c_p and c_x, it can be seen from (6) that a relatively large error of, say, $\pm 10\%$ in c_p will result in an error of only about $\pm 1\%$ in R, if R is approximately 0.90. For smaller values of R the error would be somewhat larger.

Figure 4 is a graph of the salt rejection coefficient as a function of pressure; this curve was used to yield a value of R for the conditions of the natural convection experiments.

Natural Convection Measurements

In order to simulate conditions for the natural convection model, the vessel was placed in a vertical position. Interferograms were obtained at both sets of windows in the vessel and for different values of the parameter α.

In order to compare the polarization found experimentally in the natural convection system to that computed theoretically using the mathematical model, the concentration was determined as a function of the distance normal to the membrane surface at a fixed point from the leading edge. First, the fringe shift, and thus the concentration, at a given coordinate distance x' was obtained from the interferogram as a function of the distance y' from the membrane surface. The dimensional coordinates x' and y' were then converted into the dimensionless variables x and η so that the concentration polarization θ could be plotted as a function of η for a fixed value of x, just as in (11). Such a graphical representation of the concentration profiles makes it easy to compare the theoretical and experimental results.

Unfortunately, limitations on the numerical solutions and the experimental conditions made it impossible to make such a comparison for all values of the parameters x

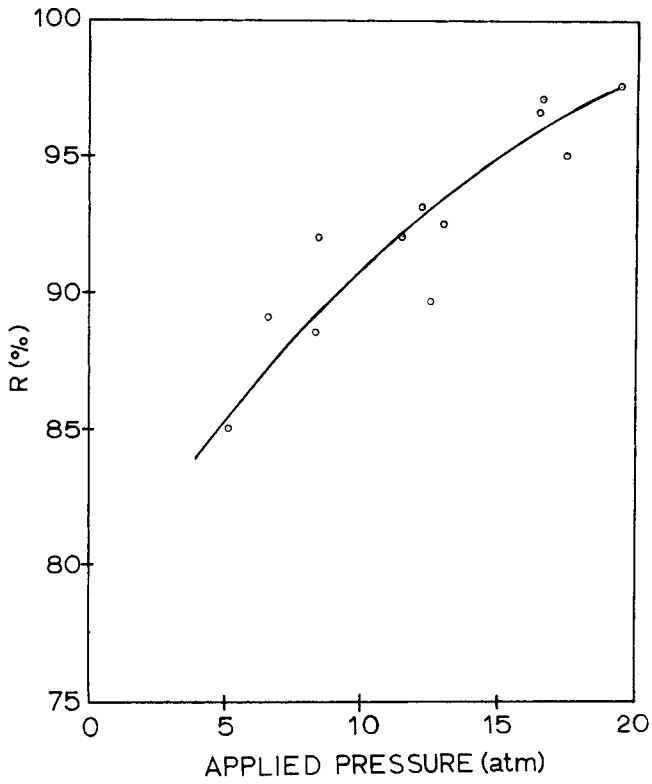

Fig. 4. Salt rejection coefficient of the membrane at various pressures.

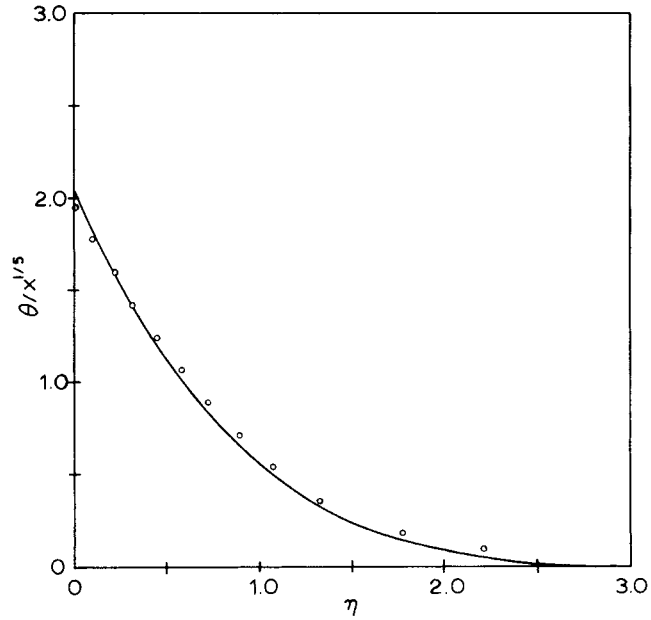

Fig. 5. Concentration profile in natural convection—top window location—$\alpha = 0.0241$, $c_x = 5.49 \times 10^{-3}$ moles/liter, $\Delta P = 10.8$ atm., $A = 1.61 \times 10^{-5}$ cm/s-atm., $x = 0.171$. ——— theoretical results for $R = 0.92$; ○ experimental results.

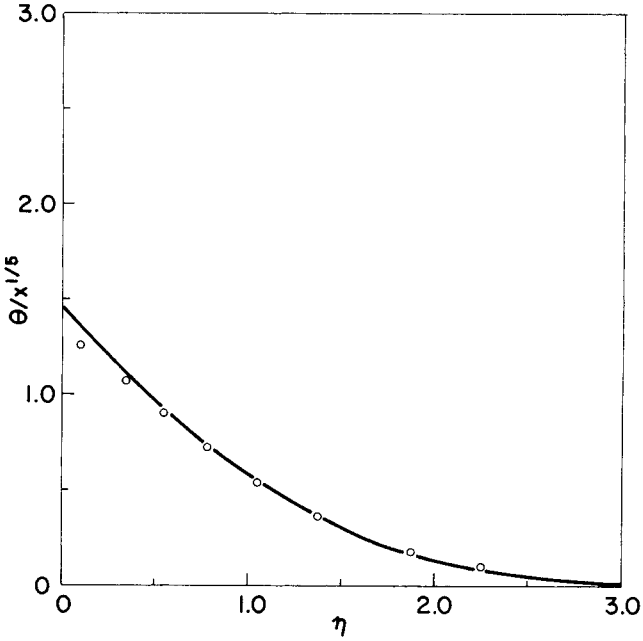

Fig. 6. Concentration profile in natural convection—top window location—$\alpha = 0.640$, $c_\infty = 4.14 \times 10^{-2}$ moles/liter, $\Delta P = 3.00$ atm., $A = 1.76 \times 10^{-5}$ cm/s-atm., $x = 2.4 \times 10^{-4}$. ——— theoretical result for $R = 0.85$; ○ experimental results.

and α. To begin with, as explained previously, it is necessary that $x >> Sc^2/N$. It is also evident from (11) that x cannot be much larger than 1 if the series is to converge. The largest value of x used in the theoretical computations was 0.79, for which the seventh term of the series (with $R = 0.92$) was found to be approximately 0.5% of the first term. It can also be seen using the table of coefficients $\phi_{m,n}$ given by Johnson and Acrivos (1969) for the case $R = 1$ that truncation of the series at the seventh term gives better than 1% accuracy if $x < 1$. On the other hand, the values of the parameter α are limited from above by experimental considerations. From its definition, $\alpha = ac_x/\Delta P = ac_x/(P_w - P_a - ac_\infty)$; hence it can be seen that α is determined by the bulk concentration of the solution used in the experiment and by the pressure applied across the membrane. However, if the concentration is too high, the fringe shift would be too large for the interferogram to be properly evaluated. Also, if the applied pressure is too small, the salt rejection would be correspondingly low (see Figure 4) and the accuracy of the values of R at these low pressures would be questionable. Conversely, the values of α are limited from below since it is necessary to keep the concentration high enough and the pressure low enough so that $x < 1.0$. Even with these restrictions it was still possible to obtain results for $10^{-6} < x < 0.8$ and for $10^{-2} < \alpha < 3$, which are respectable ranges for these parameters.

Figures 5 and 6 depict representative theoretically determined concentration profiles and the corresponding experimental results from the interferograms obtained at the top windows of the vessel (that is, the windows closest to the leading edge of the plate). The appropriate parameters for each experiment are stated in the caption for each figure. Note that the value of the salt rejection coefficient used in the numerical solution was obtained a priori from Figure 4 from a knowledge of the pressure applied across the membrane in the experiment, hence the solid curves were determined theoretically without the use of any adjustable parameters.

When using an interferometer to measure large concentration gradients, an error may be introduced due to the deflection of the light beam toward the plate, an effect which is often neglected in relating the concentration polarization to the fringe shift on an interferogram. Beach (1968) has made an extensive study of this problem in a similar situation. If the deflection of the light is severe enough, the apparent position of the plate as seen on the camera screen will tend to move with an increasing concentration gradient; also the fringe shift at any point in the diffusion layer will be affected by this deflection. Each effect will depend upon the exact plane of focus along the width of the membrane. Wachtell (1950) has developed a first-order correction for the latter effect and has shown that the error in the concentration would be given by, in the present case,

$$\delta c = \frac{Kb}{\beta^2}\left[\frac{A\Delta P c_\infty}{x^{1/5}D}\frac{\partial\theta}{\partial\eta}\right]^2\left(\frac{d}{2} - \frac{b}{6}\right) \qquad (17)$$

According to (17), the maximum error in the surface concentration for a typical natural convection test would be approximately 12% for the case in which the plane of focus was at the light beam entrance edge of the plate ($d = b$). The error would, of course, have been minimized if the focal plane were located at $d = b/3$.

In an effort to estimate the magnitude of any apparent change in the location of the plate surface resulting from the presence of a concentration gradient, the plate surface was adjusted until the maximum number of fringes were obtained. (At this point the plate would be parallel to the direction of the light beam.) The camera was then moved until the edge of the vertical plate was in focus, at which point its position was marked on the camera screen. The flow through the membrane was then stopped by plugging the exit hole for the product solution in the vessel cover. When a concentration gradient no longer existed to deflect the light beam, it was found that the plate position had not changed from its original location, hence, it was concluded that this particular source of error was absent in our case.

Any error in the measurement of the salt rejection coefficient in the batch cell configuration would have led, of course, to a corresponding error in the numerical calculations of the concentration profiles in natural convection. To illustrate this effect, Figure 7 gives the results of numerical calculations using two different values of R. The solid curve is the theoretical result with R obtained from Figure 4, whereas the dotted curve shows the effect of increasing R by about 6%, which is about twice the actual uncertainty in R from the batch cell measurements. As can be seen, the uncertainty in the value of the surface concentration is about the same as the uncertainty in R itself.

In summary then, good agreement was obtained between experiment and theory for the tests at the top window location, with an average deviation of the experimental values of the surface concentration from those predicted theoretically of only about 5%.

Figures 8 and 9 present a comparison between the numerical solutions and the experimental results taken at the bottom windows of the vessel. The agreement here is not as good as before, with the experimental data falling consistently below the theoretical curve. This is an interesting result, in view of the good agreement obtained at the top windows.

When the interference fringe pattern from the bottom window location was viewed on a screen, the pattern appeared to be wavy and unsteady. In fact, no steady state was ever achieved. Moreover, the larger the bulk concentration and applied pressure, the more frequent and intense these wavy disturbances became, and under some conditions, the flow became turbulent. These waves, which were observed to propagate in the same direction as the force of gravity when viewed on the camera screen, ap-

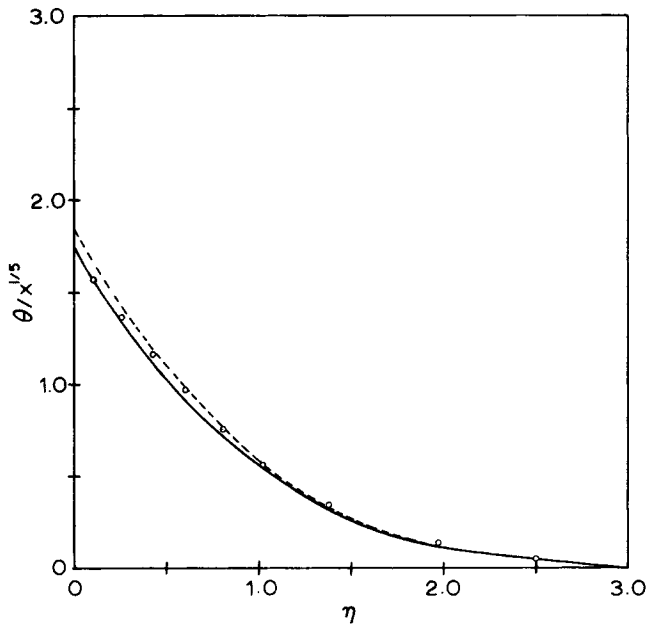

Fig. 7. Concentration profile in natural convection showing effect of the uncertainty in R—top window location—$\alpha = 0.0450$, $c_\infty = 6.45 \times 10^{-3}$ moles/liter, $\Delta P = 6.77$ atm., $A = 1.56 \times 10^{-5}$ cm/s-atm., $x = 0.0214$. ——— theoretical result for $R = 0.87$; - - - - theoretical result for $R = 0.92$; ○ experimental results.

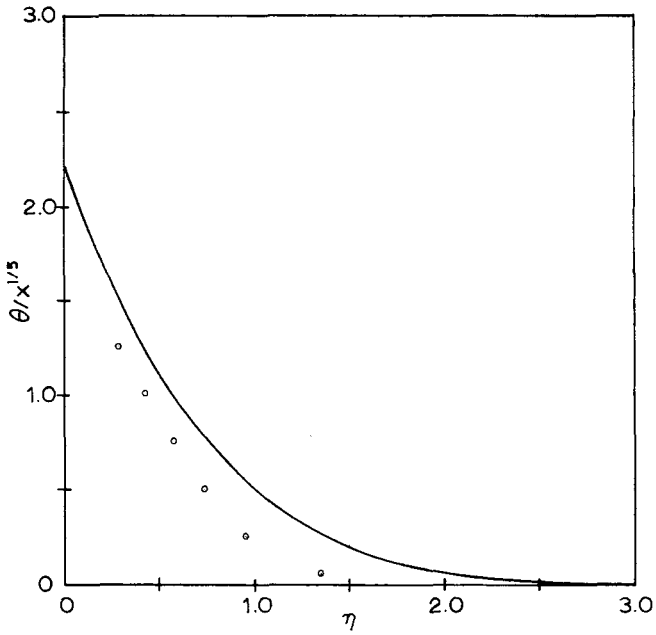

Fig. 8. Concentration profile in natural convection—bottom window location—$\alpha = 0.0245$, $c_\infty = 5.73 \times 10^{-3}$ moles/liter, $\Delta P = 11.1$ atm., $A = 1.61 \times 10^{-5}$ cm/s-atm., $x = 0.793$. ——— theoretical result for $R = 0.92$; ○ experimental results.

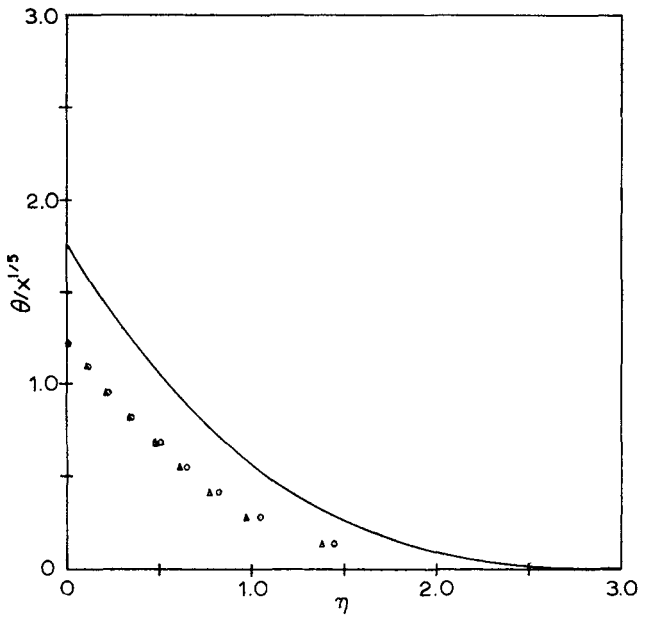

Fig. 9. Concentration profile in natural convection—bottom window location—$\alpha = 0.0922$, $c_\infty = 1.07 \times 10^{-2}$ moles/liter, $\Delta P = 5.50$ atm., $A = 1.60 \times 10^{-5}$ cm/s-atm., $x = 0.0252$. ——— theoretical result for $R = 0.87$; ○, △ experimental results at two different times indicate change in diffusion layer thickness.

parently affected the concentration polarization, as can be seen by the results in Figures 8 and 9.

For dilute salt solutions, that is $0(10^{-2})$ moles/liter or less, it was found that the overall fringe shift appeared to be constant although a change in the diffusion layer thickness was observed as the wave travelled along the plate. The concentration profiles obtained from interferograms taken at two different times are shown in Figure 9, from which it can be seen that the surface concentrations at both times are equal but that the profiles diverge for increasing η, indicating a change in the thickness of the diffusion layer.

It is likely that the buoyancy forces are such that, under certain conditions, there is a transition from the laminar flow, assumed to exist in the development of the mathematical model, to a wavy or a turbulent motion. This turbulence was most pronounced for concentrations greater than 0.1 moles/liter and pressures (ΔP) in excess of 10 atm. Of course, one would expect that the resulting increased mixing would render the concentration polarization less severe than in the corresponding case of laminar flow.

When the motion appeared highly turbulent, the wave speed of a typical disturbance was approximately 0.5 cm/s for a bulk concentration of 0.24 moles/liter and pressures, ΔP, of 5 to 10 atm. Although the flow conditions under which the data in Figures 8 and 9 were taken were hardly turbulent, the waves were visible and apparently had some effect. However, since the concentrations and pressures for which the more turbulent motions set in were too high to allow the fringe pattern to be resolved with any accuracy, the effect of any such turbulence on the concentration polarization must be inferred from the flow rate data.

Table 1 shows a comparison of the experimentally measured flow rates in the natural convection system and those calculated from (15). Clearly, this is not as sensitive a test of the model as a direct comparison of experimentally and theoretically determined concentration profiles since the flow rate is dependent on an integrated average of the surface concentration over the length of the plate. Besides, the polarization term in Equation (7) was, in most cases, too small to greatly affect the product flow rate. The agreement is, therefore, quite good, as should be expected, for those cases where the wavy motion at the bottom end of the plate should have had little effect. However, in a few cases, where the concentration was large and the polarization term in (7) was close to 1.0, the theory predicted a much lower flow rate than was measured. Under these conditions, the effect of the wavy motion seems to have been quite pronounced.

Figure 10 depicts the results of some flow rate measurements in natural convection with a large bulk concentration so that the turbulent conditions prevailed at the bottom half of the plate for large applied pressures, together with the value of Q as calculated using (15). For comparison the results of flow rate measurements taken with the same bulk concentration and the membrane in a horizontal inverted position, that is, with the membrane rejecting surface facing down, are also shown. The latter represents a gravitationally unstable configuration, with the heavier, more concentrated liquid lying above the lighter bulk solution, so that the ensuing fluid motion

Table 1. Comparison of Experimentally and Theoretically Determined Flow Rates for the Natural Convection System

P atm	c_∞ moles/liter	α	Q exp., cc/s	Q theor., cc/s
1.05	0.237	10.6	0.0267	0.0134
1.50	0.237	7.43	0.0284	0.0140
2.72	0.237	4.10	0.0352	0.0252
3.00	0.0414	0.648	0.046	0.044
4.73	0.0092	0.0913	0.072	0.072
5.65	0.0109	0.0908	0.076	0.077
5.99	0.00735	0.0577	0.089	0.084
6.71	0.0092	0.0645	0.099	0.101
6.77	0.00645	0.0448	0.088	0.092
6.80	0.237	1.64	0.058	0.052
7.22	0.00549	0.0358	0.099	0.102
8.16	0.00573	0.0330	0.113	0.115
10.3	0.0092	0.0420	0.149	0.152
10.8	0.00549	0.0239	0.147	0.151
11.1	0.00573	0.0243	0.156	0.154
15.6	0.00549	0.0166	0.210	0.216

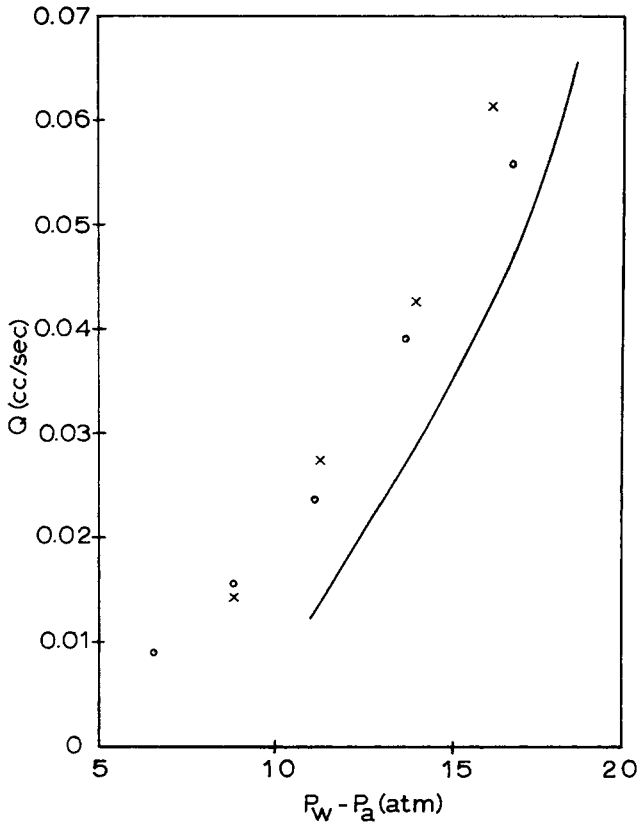

Fig. 10. Effect of natural convection instability on flow rate. c_x = 0.24 moles/liter, ac_∞ = 11 atm. ——— theoretical results from (15); ○ plate in vertical position; X plate in horizontal inverted position.

causes a decrease in the polarization near the membrane surface. The fact that, under the same operating conditions, the flow rate with the membrane in the horizontal inverted postion was found to be almost identical to that in the natural convection system indicates that the effect of the instability on the polarization is rather similar in each case.

ACKNOWLEDGMENT

The present work was initiated by a grant from the Office of Saline Water, U.S. Department of the Interior, and was supported, in part, by a grant from the Petroleum Research Fund administered by the American Chemical Society, and by a NASA Traineeship. The author is grateful to the above named organizations for this support, to Dr. Andreas Acrivos for his help and advice, to Dr. Daniel Bershader for his assistance in the design of experiments with the interferometer, and to Mr. G. E. deWerk for his excellent craftsmanship in fabricating the interferometer and its accessories.

NOTATION

A = membrane constant
a = proportionality constant relating osmotic pressure to concentration (equal to about 47 atm. liters/mole for dilute salt solutions)
b = width of vertical plate
c = solute concentration
c_s = surface concentration of solute
c_p = product concentration of solute
c_∞ = bulk concentration of solute
D = diffusivity
d = distance of plane of focus along the membrane surface to the edge of the plate where the light beam emerges from the diffusion layer
g = acceleration of gravity
h = $b\alpha R\nu N/Sc^3$
K = proportionality constant relating refractive index and concentration
L' = dimensional overall length of vertical plate
L = dimensionless overall length of vertical plate = $L'Sc^3A\Delta P/\nu N$
N = dimensionless group = $\beta g c_x \nu/(A\Delta P)^3$
P = pressure
P_w = pressure on feed or salt water side of membrane
P_a = pressure on product side of membrane
ΔP = $P_w - P_a - ac_\infty$
Q = volumetric flow rate
Q_0 = $bL'A\Delta P(1 + \alpha(1 - R))$
R = salt rejection coefficient of the membrane
Sc = Schmidt number ν/D
t = time
u' = dimensional velocity parallel to the vertical plate
u = dimensionless velocity parallel to vertical plate = $u'Sc^2/NA\Delta P$
v' = dimensional velocity normal to membrane surface
v = dimensionless velocity normal to membrane surface = $v'/A\Delta P$
v_s = dimensionless velocity normal to membrane surface at the surface of the membrane
x' = dimensional distance parallel to the vertical plate
x = dimensionless distance parallel to vertical plate = $x'Sc^3A\Delta P/\nu N$
y' = dimensional distance normal to membrane surface
y = dimensionless distance normal to membrane surface = $y'A\Delta P/D$

Greek Letters

α = dimensionless group = $ac_x/\Delta P$
β = proportionality constant relating density and concentration
η = $y/x^{1/5}$
θ = dimensionless concentration = $(c - c_\infty)/c_\infty$
θ_s = $(c_s - c_\infty)/c_\infty$
τ = dimensionless time = $v_s t/D$
ν = kinematic viscosity
τ = dimensionless time, $v_s^2 t/D$

LITERATURE CITED

Acrivos, A., "A Theoretical Analysis of Laminar Natural Convection Heat Transfer to Non-Newtonian Fluids," AIChE J., **6**, 584 (1960).

Agrawal, J. P., and S. Sourirajan, "Specification, Selectivity and Performance of Porous Cellulose Acetate Membranes in Reverse Osmosis," *Ind. Eng. Chem. Process Design Develop.*, **8**, 439 (1969).

Beach, K. W., "A Laser Interferometer for Mass Transfer Studies," M.S. thesis, UCRL—18037, Lawrence Radiation Lab., Univ. California, Berkeley (1968).

Chiu, Y., and R. M. Fuoss, "Conductance of the Alkali Halides. XII. Sodium and Potassium Chlorides in Water at 25°C.," *J. Phys. Chem.*, **72**, 4123 (1968).

Daniels, F., J. W. Williams, P. Bender, R. A. Alberty, and C. D. Cornwell, *Experimental Physical Chemistry*, pp. 473-474, McGraw-Hill, New York (1962).

Dresner, L., "Boundary Layer Buildup in the Demineralization of Salt Water by Reverse Osmosis," Oak Ridge National Lab., Tenn., ORNL Rept. 3621 (1963).

Fox, L., *Numerical Solution of Ordinary and Partial Differential Equations*, p. 160, Pergamon Press, Oxford (1962).

Gill, W. N., D. Tien, and C. Zeh, "Boundary Layer Effects in Reverse Osmosis Desalination," *Ind. Eng. Chem. Fundamentals*, **5**, 367 (1966).

Hendricks, T. J., and F. A. Williams, "Diffusion-Layer Structure in Reverse Osmosis Channel Flow," *Desalination*, **9**, 155 (1971).

Johnson, A. R., Ph.D. thesis, Stanford Univ., Stanford, California (1970).

———., and A. Acrivos, "Concentration Polarization in Reverse Osmosis Under Natural Convection," *Ind. Eng. Chem. Fundamentals*, **8**, 359, Table correction, *ibid.*, **9**, 304 (1970).

Ladenburg, R., and D. Bershader, *Interferometry. Physical*

Measurements in Gas Dynamics and Combustion, pp. 47-78, Princeton Univ. Press, New Jersey (1954).
Liu, M. K., and F. A. Williams, "Concentration Polarization in an Unstirred Batch Cell: Measurements and Comparison with Theory," *Intern. J. Heat Mass Transfer,* 13 1441 (1970).
Merten, U., "Flow Relationships in Reverse Osmosis," *Ind. Eng. Chem. Fundamentals,* 2, 229 (1963).
Raridon, R. J., L. Dresner, and K. A. Kraus, "Hyperfiltration Studies. V. Salt Rejection of Membranes by a Concentration Polarization Method," *Desalination,* 1, 210 (1966).
Sherwood, T. K., P. L. Brian, R. E. Fisher, and L. Dresner, "Salt Concentration at Phase Boundaries in Desalination by Reverse Osmosis," *Ind. Eng. Chem. Fundamentals,* 4, 113 (1965).
Sourirajan, S., *Reverse Osmosis,* Academic Press, New York (1970).
Stewartson, K., and L. T. Jones, "The Heated Vertical Plate at High Prandtl Numbers," *J. Aeronaut. Sci.,* 24, 379 (1957).
Wachtell, G. P., "Refraction Effect in Interferometry of Boundary Layer of Supersonic Flow Along Flat Plate," *Phys. Rev.,* 78, 333 (1950).

Manuscript received January 31, 1974; revision received and accepted July 8, 1974.

Three-Dimensional Flow of Fluids Through Nonuinform Packed Beds

V. STANEK

Institute of Chemical Process Fundamentals Czechoslovak Academy of Sciences, 16502 Prague, Suchdol, Czechoslovakia

and

J. SZEKELY

Department of Chemical Engineering and Center for Process Metallurgy State University of New York at Buffalo Buffalo, New York 14214

Through the statement of the Ergun equation in a vectorial form, a formulation is presented for three-dimensional flow of fluids through packed beds having a spatially variable resistance to flow. The equations were put in a form convenient for numerical solution by successive over-relaxation, and a selection of computed results is presented for cylindrical beds where the nonuniform resistance to flow obeys axial symmetry. The method outlined in the paper for calculating flow maldistribution in packed beds is thought to be a necessary first step in the representation of hot spot formation and flow nonuniformities in packed bed reactors.

SCOPE

The understanding of flow phenomena, or more specifically, flow maldistribution in packed beds having spatially nonuniform resistance to flow is of considerable practical importance in the interpretation of chemical reactor performance. In principle such flow maldistribution may occur due to spatially variable porosity or particle size distribution in the bed, or variable resistance may also be caused by radial temperature gradients in the bed. Problems of this type were discussed in two earlier papers by Stanek and Szekely (1971 and 1972) where a formulation was given by writing the axial and radial components of the Ergun equation relating pressure drop of a uniform isothermal bed to its porosity, particle diameter, and physical properties of the fluid. This procedure was shown to be only approximate by Radestock and Jeschar (1970, 1971), but the actual solution of the equations proposed by them (for two-dimensional systems) was very cumbersome.

In the present paper a statement is given of the flow problem in three dimensions by restricting the validity of the Ergun equation to an infinitesimal length of the bed and to the direction of the flow. The vectorial and differential form of the Ergun equation is then used to derive partial differential equations for the flow and pressure distributions in coordinate-free form. The handling of the equations is fully rigorous and involves no additional empiricism than that already contained in the Ergun equation. The formulation given here is thought to represent a first, necessary step for the better understanding of flow maldistribution phenomena and ultimately hot spot formation in packed bed reactors.

CONCLUSIONS AND SIGNIFICANCE

Through the statement of the Ergun equation in a differential vectorial form, equations are presented in coordinate-free form for three-dimensional fluid flow through packed beds having a distributed resistance to flow. The governing equations are developed into a form convenient for machine computation, and a selection of computed results is presented describing the velocity field and the isobar pattern in cylindrical coaxial intercommunicating beds of different resistance. Except for relatively short entrance-flow region the flow in such beds is essentially parallel (although not uniform) and a closed-form solution for the latter part is presented.

The principal significance of the work is that it provides a rigorous treatment of the Ergun equation leading to the formulation of the flow maldistribution problem as well as pressure distribution in nonuniform packings. Though strongly nonlinear, the flow equation poses no particular difficulty to the attack by numerical methods. Once the velocity pattern has been known, the pertaining pressure distribution can be obtained from a second-order partial differential equation linear in pressure also derived in the paper. All equations presented apply without a change to nonisothermal problems where heat transfer equations are coupled with the flow equations and addi-

Correspondence concerning this paper should be addressed to J. Szekely.